PLASMA ACCELERATION

I. S. SHPIGEL'

P. N. Lebedev Physics Institute, Academy of Sciences, U.S.S.R.

Submitted to JETP editor August 23, 1958

J. Exptl. Theoret. Phys. (U.S.S.R.) 36, 411-415 (February, 1959)

We consider acceleration of plasma in vacuum in an axially symmetric, inhomogeneous, pulsed magnetic field. The density of the plasma bunches is approximately 10^{12} particles/cm^3. The maximum energies for various atomic ions are as follows: nitrogen and oxygen, approximately 190 ev; helium, approximately 280 ev; hydrogen, approximately 120 ev.

1. INTRODUCTION

AT the present time the acceleration of charged-particle bunches of high density is of considerable interest. One of the means of solving this problem is the acceleration of quasi-neutral plasma bunches. In contrast with the acceleration of charged particles of one polarity, the production and acceleration of high-density plasma bunches does not require strong focusing forces. In one-shot acceleration by means of electrodynamic forces[1-5] no provisions for extended focusing are necessary.

In the present work we report on attempts to accelerate a plasma in vacuum by means of an axially symmetric, pulsed, inhomogeneous magnetic field. A measured amount of gas is admitted at a definite point in the vacuum volume. Close to this region there is a winding through which a condenser is discharged at the appropriate time. A current is induced in the gas and the acceleration forces result from the interaction of the external magnetic field with the induced current in the gas.

2. DESCRIPTION OF THE APPARATUS

The apparatus (cf. Fig. 1) consists of the vacuum chamber 1 in which the acceleration takes place, the pulsed inlet system and its feed 2, a preliminary ionization system 3, the accelerating coil and its power supply 4, and the control circuit 5.

The vacuum chamber is formed by two coaxial cylinders: the first, which is replaceable (organic glass or pyrex) is 150 mm in diameter and 500 mm long while the second, made of copper, is of the same diameter, but 700 mm long. A pressure of 2 to 4 × 10^{-5} mm Hg is maintained in the chamber. On one side the copper cylinder is covered by a replaceable brass flange which contains vacuum gaskets for the various probe inputs. The other end is made from a glass cylinder. On the other side the
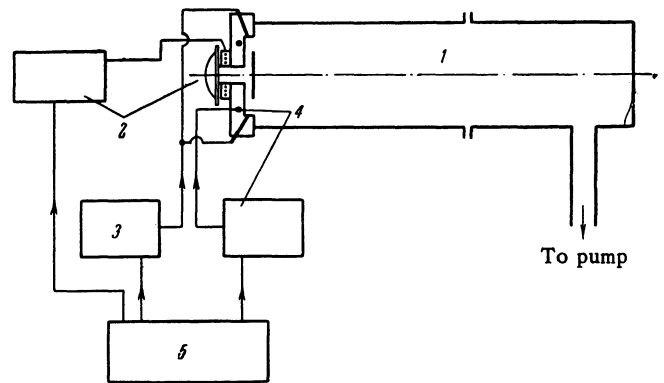

FIG. 1. Block diagram of the apparatus.

glass cylinder there is a flange of organic glass. On this flange (cf. Fig. 2) are mounted the pulsed gas inlet 1 (an electromagnetic valve[6]), the preliminary ionization electrodes 2, the accelerating winding 3, and a disc that provides better distribution of the gas flow 4.

The accelerating coil is cemented inside the disc of organic glass. In these experiments the winding is a single turn. At time t_2, an IM 2.7-50 condenser is discharged through the winding by means of a spark gap. The voltage, U, to which the condenser is charged, varies between 10 and 24 kv. The frequency of the oscillations which re-
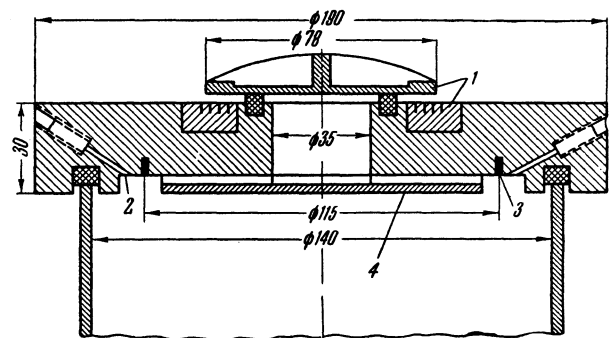

FIG. 2 Cross section of the organic-glass flange.

FIG. 3. High-speed photograph showing the motion of the plasma in air. The vertical scale is $\Delta z = 11.5$ cm along the z axis $\tau = 280 \mu$sec. a) $U_c = 14.5$ kv; b) $U_c = 22.5$ kv.

sult when the condenser is discharged through the single turn is approximately 120 kc/sec; the discharge is a damped oscillatory discharge.

All the elements in the system are operated in a definite time sequence which is determined by a control circuit. At time t_1 the valve opens. The preliminary ionization system is also turned on; this unit is a 500-watt rf generator which operates at 15 Mcs. After a controlled time interval τ, at time t_2 (when the required gas pressure is established near the accelerating coil) the rf generator is turned off and the voltage is applied to the accelerating coil, initiating acceleration of the plasma. A slave sweep on the oscilloscope which is used for observation is triggered by the control circuit 1.5 microseconds before the voltage is applied to the accelerating coil.

3. EXPERIMENTAL RESULTS

The following have been investigated: the plasma velocity along the acceleration axis (the z axis), the nature of the radial motion, the velocity of the wave front, and the relation between pulse duration and plasma density.

FIG. 4. High-speed photograph of the plasma pressure in helium along the z axis. $\Delta z = 11.5$ cm; $U_c = 22.5$ kv. a) $\tau = 220 \mu$sec, b) $\tau = 280 \mu$sec, c) $\tau = 400 \mu$sec.
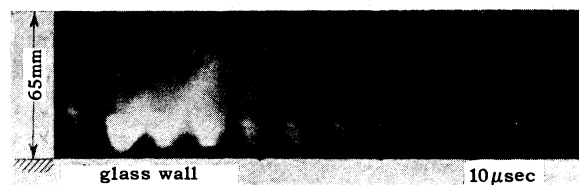

FIG. 5. High speed photograph showing the radial motion of the plasma in air. $U_c = 22.5$ kv, $\tau = 280 \mu$sec.

(a) Motion of the Plasma Along the Z Axis and Radial Motion

These measurements are carried out by high-speed photography of the luminous plasma, with a CFR-2M camera. To record the motion of the plasma along the acceleration axis the slit of the camera (0.5 cm wide) is oriented along the z axis. The length of the slit, taken from the accelerating coil, is 11.5 cm.

Figure 3 shows typical photographs obtained with air. The sharply defined luminescent plasma bursts are easily distinguished on these photographs. The periodic expulsion of plasma from the acceleration region takes place at twice the frequency of the oscillations in the accelerating turn. The existence of an initial velocity component causes the plasma to collide with the wall of the vacuum chamber at a distance of 4 or 5 cm from the accelerating turn. As a result the plasma velocity in the z direction is reduced (the break in the luminescent band in Fig. 3b).

When the time interval τ is increased a still greater deceleration effect is noted. Figure 4 shows photographs of the motion of a helium plasma in the z direction taken with various values of τ. With $\tau = 280 \mu$ sec (Fig. 4a) there is almost no deceleration whereas when $\tau = 400 \mu$ sec (Fig. 4c) the effect is very large for the initial bursts. Apparently this phenomena is due to the presence of high-density gas in front of the moving plasma. The first pulses remove the gas in front of the plasma so that there is no significant deceleration for subsequent pulses.

Initially the luminescent intensity increases from pulse to pulse; then it falls off. This effect is due to the enhanced conditions for discharge development (the increasing number of free electrons in the discharge region) and the reduction in the amplitude of the oscillations in the accelerating coil. Optimum conditions obtain at about the third or fourth expulsion of the plasma.

The velocity is a maximum for the initial pulses since the accelerating field is large initially and the plasma mass is still small because of incomplete ionization. Later the ionization increases but the currents in the winding and in the plasma have fallen off.
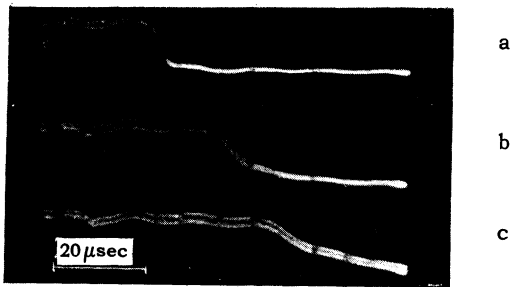
FIG. 6. Pulses at the rf probes for different distances between the probe and the accelerating coil. Plasma in air, $U_c = 18$ kv, $\tau = 280 \mu$sec. a) $\Delta z = 21$ cm, b) $\Delta z = 51$ cm, c) $\Delta z = 76$ cm.

Figure 5 shows a high-speed photograph of the radial motion of the plasma. The picture was taken through a radial slit 0.5 cm wide. As is apparent from Fig. 5, in addition to having a v_z component the plasma has a v_r component directed away from the center. After the plasma collides with the wall of the vacuum chamber, v_r changes in both magnitude and direction. Similar photographs are obtained with hydrogen; no significant differences are observed.

This same method is used to measure the velocity of the luminous plasma front; this velocity is related to some effective particle velocity.

The energy of the nitrogen and oxygen ions (air input) obtained from measurements of the corresponding photographs is found to be 80 — 190 ev; for hydrogen and helium ions the range is 40 — 120 ev and 120 — 280 ev, respectively.

(b) Velocity of the Front and Pulse Duration for a Plasma of Given Density.

These measurements are made by means of an rf probe which is sensitive to plasma in the density range from 10^{11} to 10^{13} cm^{-3} and a waveguide which measures plasma densities of 10^{12} cm^{-3}.

The rf probe consists of an inductance circuit which is weakly coupled to a low-power rf oscillator. The tank circuit is tuned to the oscillator frequency. When there is a conducting medium (plasma) inside or outside the probe, the rf eddy currents that arise in the circuit effectively reduce the inductance of the probe and shift the resonant frequency of the circuit toward higher frequencies. As a result of this detuning, the voltage is reduced. The time behavior of the voltage is displayed on an oscilloscope.

The velocity of the plasma front is measured with two rf probes separated by a known distance. One probe is generally kept fixed while the second is moved along the z axis. The velocity is determined from the known distance Δz and the meas-
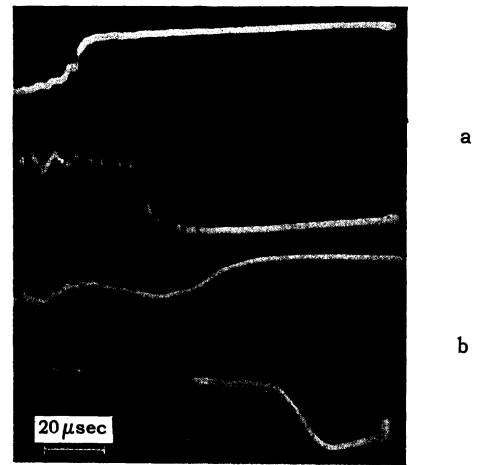

FIG. 7. Change of the pulse shape at the rf probe and starting time as a function of delay time τ and distance from the accelerating coil Δz. Plasma in air, $U_c = 20$ kv, first probe probe, $\Delta z = 15$ cm, second probe, $\Delta z = 33$ cm. a) $\tau = 310 \mu$sec, b) $\tau = 400 \mu$sec.

ured time interval ΔT corresponding to the difference in arrival time at the probes. In this case it is possible to determine the velocity of a front for a given density.

A series of oscillograms taken with these probes is shown in Fig. 6. It is apparent that as the distance from the accelerating coil is increased the time delay required for the excitation of the mobile probe increases, the signal front shows more slope, and the amplitude of the signal is reduced. The minimum plasma density which the probe can record is $n_{min} \simeq 10^{11}$ cm^{-3}. The mean plasma velocity, computed from this oscillogram, is approximately 3×10^6 cm/sec. The discrepancy in the velocity measurements by high-speed photographs and rf probes indicates a velocity dispersion effect.

Figure 7 are shows oscillograms of the pulses from the two rf probes taken with air using two different delay times. The pulses in Fig. 7b slope more, start later and the time interval between them is much larger than in Fig. 7a. Similar results, obtained in helium, are shown in Fig. 8. Here the shift of the pulses for both the first and second probes are clearly apparent and the shift of the second probe is much larger. The deceleration effect in helium and hydrogen is much stronger than in air; this is explained by the different thermal velocities of the gases and the resulting higher pressure of the gas in front of the moving plasma for the same values of τ.

Experiments have also been carried out to verify the expulsion of plasma from the acceleration region in individual bunches (density modulation of the plasma as a function of time). However, no density modulation was observed at the discharge frequency,
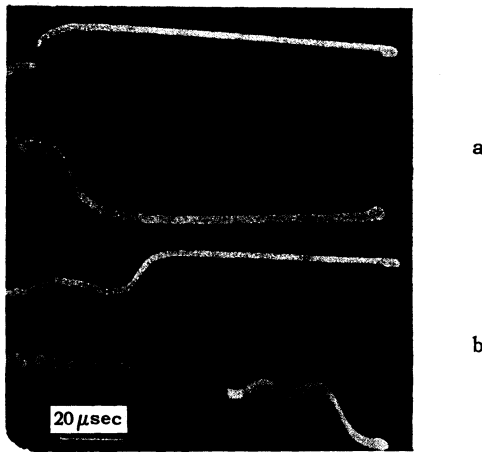
FIG. 8. Change of pulse shape at the rf probe and time of excitation as a function of delay time τ and distance from the accelerating turn. Plasma in helium, $U_c = 20$ kv, distance of the probe to the accelerating turn the same as in Fig. 7.
a) $\tau = 190\,\mu$sec, b) $\tau = 280\,\mu$sec.

120 kcs. Apparently this is due to the considerable velocity spread of the ions inside the bunches. The frequency of the oscillations in the accelerating col was then reduced to 56 kcs by increasing the capacity of the condenser. In Fig. 9 are shown oscillograms of the voltage in the rf probe before and · after detection and the voltage in the accelerating coil. In the second part of both oscillograms there is visible a clearly defined amplitude modulation of the rf voltage in the probe, indicating a density modulation of the plasma as a function of time at the probe position. At larger value of z the modulation cannot be seen because of the spread in velocity. There is no modulation in the first part of the pulse from the probe because a minimum density $n_{min} > 10^{13}$ cm^{-3} is required for modulation to be observed.
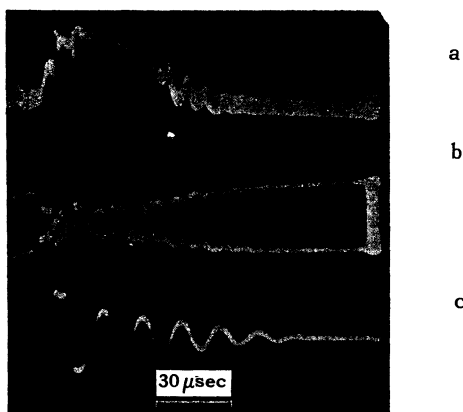

FIG. 9. Oscillogram showing the voltage at the rf probe for motion of the plasma in air with density modulation. $U_c = 15$ kv, $\tau = 260\,\mu$sec. a) voltage at the probe after detection, b) before detection, c) voltage oscillogram for the accelerating coil, $f = 58$ kcs.
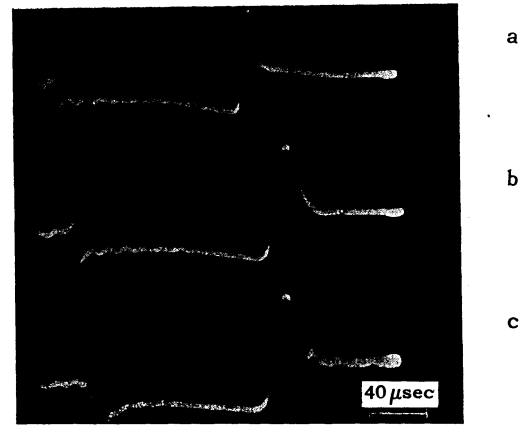

FIG. 10. Detector current pulses from a "radiating" waveguide as a function of distance from the accelerating coil Δz. Plasma in air, $U_c = 20$ kv. a) $\Delta z = 13.5$ cm, b) Δ b) $\Delta z = 34.5$ cm, c) $\Delta z = 56$ cm.

The slope of a given signal front from the rf probe makes it difficult to determine the length of the pulse from a plasma of given density. For this reason a "radiating" waveguide is used. The use of a waveguide in these measurements is based on reflection of radio waves from a plasma when the frequency of the external field is lower than the natural plasma frequency $\omega_0 \sim n^{1/2}$.

The sealed end of the waveguide is introduced inside the chamber. When there was no plasma in the waveguide it was possible to observe a stationary standing-wave distribution due to reflection from the open end. When the plasma appears the radiation is reduced and the standing wave distribution changes. The change in the detector current (proportional to field intensity at any point in the waveguide) is presented on the screen of an oscilloscope. In these measurements the waveguide is driven at 9.4×10^9 cps, corresponding to a plasma density for which total reflection obtains at $n = 10^{12}$ cm^{-3}.

In Fig. 10 are shown oscillograms of plasma pulse lengths for a plasma with $n \geq 10^{12}$, as a function of distance z. The leading edge of the pulse on the last oscillogram exhibits smearing. This is apparently due to the fact that in these measurements the waveguide was located inside a metal tube and there was multiple reflection. The dependence of plasma pulse length on the coordinate z obtained in this work is shown in Fig. 11.
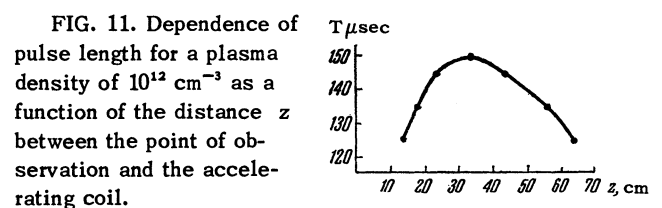
FIG. 11. Dependence of pulse length for a plasma density of 10^{12} cm^{-3} as a function of the distance z between the point of observation and the accelerating coil.

We wish to take this opportunity to thank V. I. Veksler, M. S. Rabinovich, and L. M. Kovrizhnykh for a discussion of the results of the experiment, E. D. Andryukhin for help in carrying out a number of measurements, and E. A. Smirnov for construction of the apparatus.

[1] W. H. Bostick, Phys. Rev. **104**, 292 (1956).

[2] A. C. Kolb, Phys. Rev. **107**, 345 (1957).

[3] L. A. Artsimovich et al., J. Exptl. Theoret. Phys. (U.S.S.R.) **33**, 3 (1957), Soviet Phys. JETP **6**, 1 (1958).

[4] A. I. Morozov, J. Exptl. Theoret. Phys. (U.S.S.R.) **32**, 305 (1957), Soviet Phys. JETP **5**, 215 (1957).

[5] G. S. Janes, Bull. Am. Phys. Soc. **3**, 85 (1958).

[6] I. O. Shpigel', Приборы и техника эксперимента (Inst. and Meas. Engg.) (U.S.S.R.) 1, 1959 (in press).